

Kinetics of the aerosol formation at 193-nm photolysis of 1.4-cyclohexadiene–NO–air mixture

S.N. Dubtsov, E.N. Chesnokov, and L.N. Krasnoperov*

*Institute of Chemical Kinetics and Combustion,
Siberian Branch of the Russian Academy of Sciences, Novosibirsk, Russia
* New Jersey Institute of Technology, Newark, NJ, USA*

Received November 28, 2001

A new experimental technique has been developed for direct time-resolved studies of the kinetics of aerosol formation. It is based on a combination of pulsed excimer laser photolysis and space- and time-resolved monitoring of scattered light with a gated intensified CCD camera. The experimental setup allowed detection of aerosol particles more than 45–50 nm in diameter and with the number concentration ranging from $3 \cdot 10^6$ to $6 \cdot 10^8$ particles/cm³. The time range of aerosol formation kinetics was from 10^{-7} to 10^{-2} s. Kinetics of photochemically induced aerosol formation in 1.4-cyclohexadiene–NO–air mixture was studied. The evolution of the particle number concentration and the size distribution was investigated, as well as the increase in the scattered light intensity depending on a delay after the photolyzing pulse. Quantum yield of aerosol products was estimated to be in the range from 10^{-2} to 2%, which is comparable with the values characteristic of organic aerosols.

Introduction

Formation of the submicron fraction of atmospheric aerosol has attracted considerable attention in recent decade (see, for example, Refs. 1 and 2). Nevertheless, many aspects of this problem are poorly studied yet. Organic compounds make, on the average, up to 30–50% of the submicron aerosol fraction. A significant part of the organic component is formed due to photooxidation of unsaturated and aromatic hydrocarbons in the presence of nitrogen oxides NO_x. Low-volatile products (aldehydes, mono- and dicarboxylic acids, nitroethers, peroxyalkylnitrates, and others³) transit into the aerosol phase. These processes occur against the background of numerous gas-phase reactions. The fraction of products that transit into aerosols depends on the concentration of initial reagents and varies from 10^{-2} to several percent of reacted organic precursors.^{3,4}

It is rather difficult to study the mechanisms of photochemical aerosol formation in the actual atmosphere, therefore photonucleation of organic compounds is mostly studied in smog chambers under conditions imitating, to some or other degree, the polluted atmosphere (see, for example, Ref. 4). In such experiments, particles larger than 0.1 μm are usually detected. Thus, the information about the aerosol formation at the initial stages, which are most sensitive to previous gas-phase processes, is usually lost. The approach proposed in this paper allows direct determination of the concentration and size spectrum of nanometer aerosols.

1. Experiment

An experimental setup to study the photochemical aerosol formation kinetics consists of the following

main parts: a photolyzing ArF laser ($\lambda = 193$ nm, $t = 10$ ns, $E_p = 40$ –80 mJ), a sensing KrF laser ($\lambda = 248$ nm, $t = 10$ ns, $E_p = 10$ –18 mJ), a flow-through microreactor, a high-sensitivity digital video camera, and a gas system for creation of reagent flows (Model 5580E, Brooks). Figure 1 depicts schematically the aerosol microreactor, geometry of the photolyzing and sensing laser beams, and a recording system.

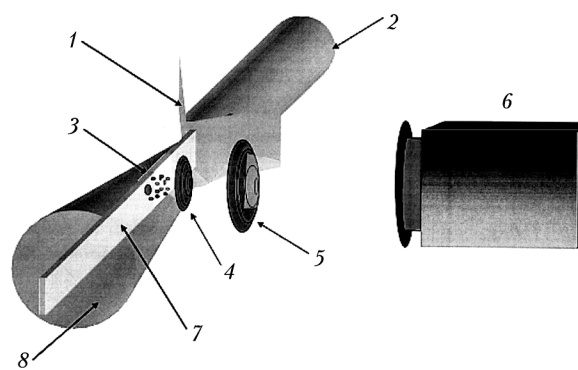


Fig. 1. Layout of the central part of the aerosol reactor: 150×20 μm rectangular slit 1, sensing KrF laser beam ($\lambda = 248$ nm) 2, reactor counting volume 3, second focusing lens (diameter of 25.4 mm, $f_{248} = 200$ mm) 4, high-sensitivity digital camera 5, first focusing lens (diameter of 6.25 mm, $f_{248} = 8.2$ mm) 6, rectangular sensing beam cut out by the slit 7, photolyzing beam of ArF laser ($\lambda = 193$ nm) 8.

The optical slit forms a thin rectangular sensing beam ($\approx 20 \times 150$ μm) inside a large cone of the photolyzing beam. The counting volume is determined by the layer thickness and the objective's field of view. This volume was varied within $(1-3) \cdot 10^{-7}$ cm³ by changing the slit width. The objective (magnification factor of 78 ± 5) directs the scattered light into the digital camera. After each laser pulse, the image of the

counting volume (frame) is recorded in a single file. The lasers and the camera are switched on by a master oscillator allowing variation of the delay Δt between the photolyzing and the sensing pulses from 10^{-7} to 10^{-2} s. The repetition frequency of the photolyzing and sensing pulses was 1 Hz.

The use of a high-sensitivity TV camera for detection of submicron aerosols was described in Ref. 7 for a continuous-wave source of sensing radiation.

A specialized algorithm was developed to separate the light scattered by individual aerosol particles in a frame. With this approach, we determined the concentration of aerosol particles, intensity of scattered light, and integral light scattering from the whole counting volume. The sensitivity of the recording system was calibrated before and after every experiment using polystyrene latex (PSL) aerosol particles. The working volume of these particles was sprayed with a sprayer (TSI, 3079). The resulting aerosol particles then passed through the reactor. Since the size of the particles under study is less than the sensing radiation wavelength, the aerosol particle diameter D_a was determined as $D_a = (I_a/I_{\text{PSL}})^{1/6} \times 73 \text{ nm}$, where I_a is the intensity of light scattered by a particle, and I_{PSL} is the intensity of the light scattered by a latex particle 73 nm in diameter. Additional experiments showed that this technique allows detection of particles more than 50 nm in diameter. The measurable concentration ranged roughly from $3 \cdot 10^6$ to $6 \cdot 10^8$ particle/cm³. The minimum concentration of particles is determined by the counting volume and the need in accumulation of a large number of frames. The maximum concentration is limited by particle overlap in a frame.

2. Results and discussion

The typical concentrations of the reagents in the experiments had the following values: 1,4-cyclohexadiene [C_6H_8] = $1.50\text{--}2.50 \cdot 10^{17}$, [NO] = $0\text{--}9 \cdot 10^{17}$, [O_2] = $3.10\text{--}3.70 \cdot 10^{18}$ molecule/cm³. The photolyzing light intensity at the center of the reactor varied from $2.2 \cdot 10^{16}$ to $3.0 \cdot 10^{16}$ photon/cm², and the sensing light intensity was within $(3.7\text{--}7.5) \cdot 10^{16}$ photon/cm².

The dependence of the particle number concentration and size distribution on the delay between the photolyzing and sensing laser pulses Δt was studied. Figure 2 shows typical time behavior of the particle size distribution. A typical feature of all experiments is also the fact that at short Δt there are no aerosol particles, then a small number of fine particles arise, and large particles are formed only after some Δt . The concentration of these particles increases with Δt , but the size does not grow. Particles of intermediate size are absent.

Similar behavior of the particle size distribution was observed earlier for other organic systems: at pulsed photochemical initiation of toluene oxidation⁵ and at continuous photolysis of chlorobenzene in air.⁶ In Ref. 6 it was found that the photoaerosol size distribution

had two modes (modal diameters about 7 and 50 nm). The increase of the photolysis time led to the increase of the particle number concentration and to the growth of the fraction of larger particles, while the modal size did not change. This behavior is most probably caused by particle evaporation. Analogous effect of evaporation on the particle size distribution was demonstrated in some numerical experiments (see, for example, Ref. 8).

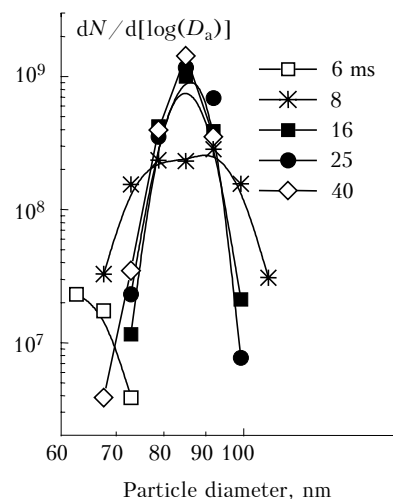


Fig. 2. Time dependence of the particle size distribution after the photolyzing ArF laser pulse: [C_6H_8] = $1.95 \cdot 10^{17}$, [NO] = $1.387 \cdot 10^{17}$, [O_2] = $3.163 \cdot 10^{18}$ molecule/cm³. The photolyzing pulse intensity of $2.9 \cdot 10^{16}$ photon/cm².

Figure 3 depicts typical dependence of the particle number concentration on the delay time. The photolyzing radiation intensity I_0 ($\lambda = 193 \text{ nm}$) in this experiment was $2.9 \cdot 10^{16}$ photon/cm². The absorption cross section measured by us at this wavelength σ_{193} for 1,4-cyclohexadiene was equal to $3.66 \cdot 10^{-18} \text{ cm}^2$. Thus, the amount of absorbed quanta I_{abs} calculated as $I_{\text{abs}} = I_0 (1 - \exp(-N\sigma l))$, where N is the concentration of the absorbing substance, σ is absorption cross section, and l is the thickness of the absorbing layer, was equal to $(1.46\text{--}1.48) \cdot 10^{16}$ photon/cm³. At the photolysis ($\lambda = 193 \text{ nm}$), quantum yield equal to unity for the overwhelming majority of olefins, we obtain about $1.47 \cdot 10^{16}$ molecule/cm³ of photolysis products (N_{phot}) for every laser pulse. Assuming the molecular weight of the products forming the aerosol (so-called monomers) to be equal to 110 g/mol (the sum of molecular weights of C_6H_8 and NO) and the density equal to 0.8 g/cm^3 , we obtain the monomer volume of $2.08 \cdot 10^{-22} \text{ cm}^3$. Using this value and having known the particle size distribution and the number concentration, we can calculate the concentration of monomers in aerosol N_{mon} and then the quantum yield of the aerosol formation $\phi_a = N_{\text{mon}}/N_{\text{phot}}$. For data presented in Fig. 3, ϕ_a is close to 10^{-2} what is comparable with the data from Ref. 3. The value of ϕ_a was determined as ranging from $5 \cdot 10^{-4}$ to $2 \cdot 10^{-2}$ for the whole range of the studied concentrations of C_6H_8 and NO.

No correlation was found between the quantum yield of aerosol formation and concentration of reagents.

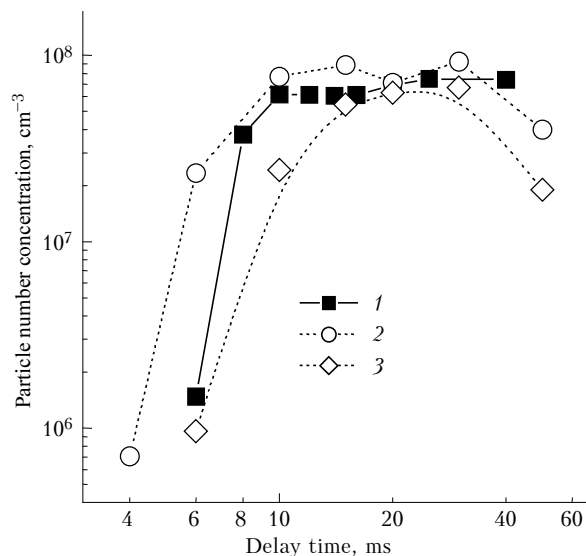


Fig. 3. Aerosol particle number concentration as a function of the delay time: $[C_6H_8] = 1.910 \cdot 10^{17}$, $[NO] = 6.157 \cdot 10^{17}$, $[O_2] = 3.10 \cdot 10^{18}$ molecule/cm³, N₂ – up to 1 atm (1); $[C_6H_8] = 1.938 \cdot 10^{17}$, $[NO] = 2.973 \cdot 10^{17}$, $[O_2] = 3.144 \cdot 10^{18}$ molecule/cm³, N₂ – up to 1 atm (2); $[C_6H_8] = 1.95 \cdot 10^{17}$, $[NO] = 0$, $[O_2] = 3.163 \cdot 10^{18}$ molecule/cm³, N₂ – up to 1 atm (3).

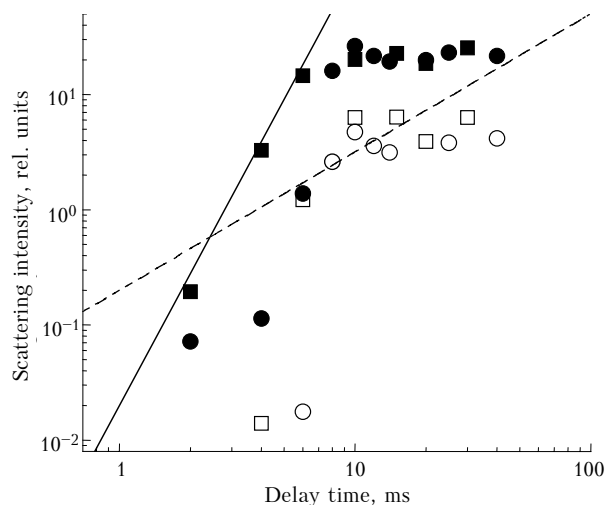


Fig. 4. Scattered light intensity as a function of the delay time. Squares: $[C_6H_8] = 1.910 \cdot 10^{17}$, $[NO] = 6.157 \cdot 10^{17}$, $[O_2] = 3.10 \cdot 10^{18}$ molecule/cm³, N₂ – up to 1 atm; circles: $[C_6H_8] = 1.938 \cdot 10^{17}$, $[NO] = 2.973 \cdot 10^{17}$, $[O_2] = 3.144 \cdot 10^{18}$ molecule/cm³, N₂ – up to 1 atm; close signs corresponds to the total scattering intensity, open signs correspond to the intensity of radiation scattered only by aerosol particles; theoretical dependence $I_{scatt} \propto \Delta t^{6/5}$ (dashed line) and power dependence $I_{scatt} \propto \Delta t^{3.9}$ (solid line).

Besides the dynamics of particle number concentration and the size spectrum, we studied the

dependence of the scattered radiation intensity I_{scatt} on Δt (Fig. 4). Unlike the theoretically predicted dependence $I_{scatt} \propto \Delta t^{6/5}$ (see, for example, Ref. 9), the observed exponent varied from 3 to 3.9 at small Δt . At Δt larger than 10 ms, I_{scatt} is almost independent of the delay. As can be seen from Fig. 4, the experimental data do not agree with the theoretical dependence in the whole range of Δt . The closed signs in Fig. 4 are for the total scattering, and open ones are for the intensity of radiation scattered only by aerosol particles. Particles are responsible for only 20 to 30% of scattered radiation. The rest radiation may be scattered by smaller particles, not identified as particles.

Conclusions

In this paper we have reported a new experimental technique for studying the kinetics of photochemical aerosol formation, which detects particles larger than 45–50 nm in diameter with the number density ranging from $3 \cdot 10^6$ to $6 \cdot 10^8$ particle/cm³. Our experimental setup allows the aerosol formation kinetics to be studied in the time range from 10^{-7} to 10^{-2} s.

Using the proposed technique, we have studied kinetics of the aerosol formation at pulsed laser photolysis ($\lambda = 193$ nm) of 1,4-cyclohexadiene–NO–air mixtures. The dependence of the number concentration and size spectrum of aerosol particles on the delay between the photolyzing and the sensing laser pulses Δt has been studied. The quantum yield of aerosol formation has been determined to vary from $5 \cdot 10^{-4}$ to $2 \cdot 10^{-2}$ depending on the reagent concentration.

The abnormal dependence of scattered radiation intensity on Δt has been found.

References

1. B.J. Finlayson-Pitts and J.N. Pitts, Jr., *Atmosph. Chem.: Fundamentals and Experimental Technique* (John Wiley, New York, 1986), 1098 pp.
2. J.H. Seinfeld, *Atmospheric Chemistry and Physics of Air Pollution* (John Wiley, New York, 1986), 738 pp.
3. D. Grosjean and S.K. Friedlander, in: *Character and Origin of Smog Aerosols*, ed. by M. Hidy (John Wiley, New York, 1979), pp. 435–473.
4. P.H. McMurry and D. Grosjean, *Atmos. Environ.* **19**, No. 9, 1445–1451 (1985).
5. R.S. Carlsson, J.J. Szente, J.C. Ball, and M.M. Maricq, *J. Phys. Chem. A* **105**, No. 1, 83–89 (2001).
6. S.N. Dubtsov, K.P. Koutzenogii, A.I. Levykin, and G.I. Skubnevskaya, *J. Aerosol Sci.* **26**, No. 4, 705–716 (1995).
7. R.A. Mavliev, A.N. Ankilov, and K.P. Koutzenogii, *Dokl. Akad. Nauk SSSR* **258**, No. 6, 1357–1359 (1981).
8. N.P. Rao and P.H. McMurry, *Aerosol Sci. Technology* **11**, No. 1, 120–134 (1989).
9. H.L. Green and W.R. Lane, *Particulate Clouds: Dusts, Smokes, and Mists* (E. & FN Spon, London, 1964).